

7-16-2014

Methods of Increasing Net Work Output of Organic Rankine Cycles for Low-Grade Waste Heat Recovery

Brandon J. Woodland
Purdue University, bwoodlan@purdue.edu

James E. Braun
Purdue University, jbraun@purdue.edu

Eckhard A. Groll
Purdue University, groll@purdue.edu

W Travis Horton
Purdue University, wthorton@purdue.edu

Follow this and additional works at: <http://docs.lib.purdue.edu/herrick>

Woodland, Brandon J.; Braun, James E.; Groll, Eckhard A.; and Horton, W Travis, "Methods of Increasing Net Work Output of Organic Rankine Cycles for Low-Grade Waste Heat Recovery" (2014). *Publications of the Ray W. Herrick Laboratories*. Paper 104. <http://docs.lib.purdue.edu/herrick/104>

This document has been made available through Purdue e-Pubs, a service of the Purdue University Libraries. Please contact epubs@purdue.edu for additional information.

Methods of Increasing Net Work Output of Organic Rankine Cycles for Low-Grade Waste Heat Recovery

Brandon J. WOODLAND^{1*}, James E. BRAUN¹, Eckhard A. GROLL¹, and W. Travis HORTON¹

¹Purdue University
School of Mechanical Engineering
Ray W. Herrick Laboratories
West Lafayette, Indiana, USA
Email: bwoodlan@purdue.edu

* Corresponding Author

ABSTRACT

In heat engine design, the usual objective is to maximize thermal efficiency. However, for heat engines applied to waste heat recovery, an appropriate objective is to maximize power production by converting as much of the waste heat as possible into work. An organic Rankine cycle (ORC) is particularly well-suited to waste heat recovery because of its compactness relative to a steam Rankine cycle at typical waste heat temperatures. For a single-phase (sensible) waste heat stream with a finite capacity, maximization of thermal efficiency does not result in maximum power production. Therefore, traditional approaches aimed at increasing cycle thermal efficiency are not helpful. Instead, it is necessary to find designs that properly balance heat extraction from the source and thermal efficiency of the heat engine. In this regard two alternative ORC configurations are studied and compared using a uniform modeling strategy. These configurations are the ORC with two-phase flash expansion and the ORC with zeotropic working fluid mixture (ZRC). There are two key elements of the modeling strategy. Pinch point temperature differences are used to characterize the heat exchangers, and the air-side condenser fan power requirements are estimated. Each cycle configuration is modeled and compared to a baseline ORC for a range of potential working fluids and source fluid temperatures.

Based on the model, the ORC with flash expansion shows the most consistent improvement over the baseline ORC. The highest increase in net power of 84% over the baseline is seen at the low source temperature of 80 °C with water as the working fluid. However, this cycle and working fluid present more costly challenges to implementation, particularly in the expander design. This is due to the high volume ratios needed to expand low-pressure, two-phase water. The ZRC gives some of the highest relative improvements, but only when condenser fan power consumption is high. For a 100 °C source temperature and a mixture of R134a and R245fa as the working fluid, an improvement of 92% over the baseline is seen if the required condenser fan power is 846 W/(m³/s). In addition, the ZRC has the benefit that it can utilize existing ORC expanders, giving it a potentially lower cost than the ORC with flash expansion. These results are valid in terms of their comparison of the thermodynamic potential of the different cycles and working fluids. However, a more detailed analysis incorporating the geometry and cost of each component is necessary to arrive at a final recommendation for a given application.

1. INTRODUCTION

The traditional objective in the design of heat engines is to maximize thermal efficiency. In other words, heat engines are often designed to produce the required amount of work from the smallest heat input possible. However, for heat engines used in waste heat recovery applications, the design problem is slightly different. A waste heat source is available at a given rate and will be discarded whether it is used or not. For conversion of waste heat to power, an appropriate objective is to convert as much energy in the waste-heat stream as possible into work. This is the objective considered in the present study.

A particular heat engine design that is well-suited to this objective is an organic Rankine cycle (ORC). The working fluid in a typical ORC follows the same processes as steam in a traditional Rankine cycle. However, the ORC

working fluid is typically an organic compound, such as a hydrofluorocarbon refrigerant or a hydrocarbon. Such working fluids are favored over steam when low-grade heat sources (with temperatures ranging from 80 °C – 300 °C) are used because they allow for higher condensing pressures, lower pressure ratios, a smaller expander, and better heat source temperature matching than steam. An ORC is shown schematically in Figure 1. A process diagram is shown in Figure 2, in which the temperature profiles of heat source and heat sink fluids having properties of atmospheric air are superimposed on the temperature-entropy plane of the ORC working fluid.

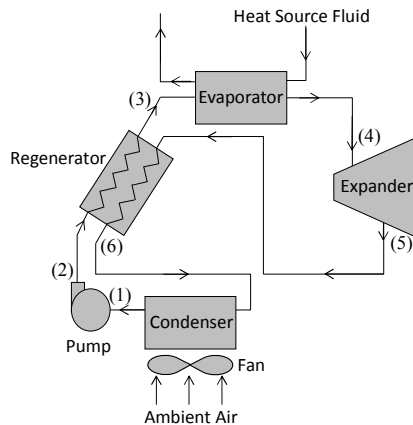


Figure 1: Schematic representation of an air-cooled ORC with optional internal regenerator. All cycle configurations in the present work follow this schematic.

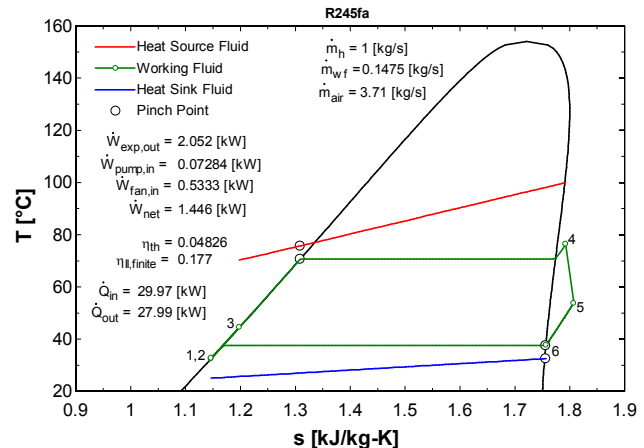


Figure 2: Process diagram for a traditional (baseline) ORC. Parameters are optimized for maximum net work production. The heat source fluid inlet temperature is 100 °C. Volume-specific cooling fan power is 168 W/(m³/s). Labeled state points correspond to Figure 1.

When the waste-heat stream is a single-phase fluid, it cools as heat is transferred from it to the ORC. Under these conditions maximization of thermal efficiency does not result in maximum power production from the heat source. Therefore, many typical approaches to Rankine cycle efficiency enhancement do not apply. This can be seen by comparing the process diagrams in Figures 3 and 4.

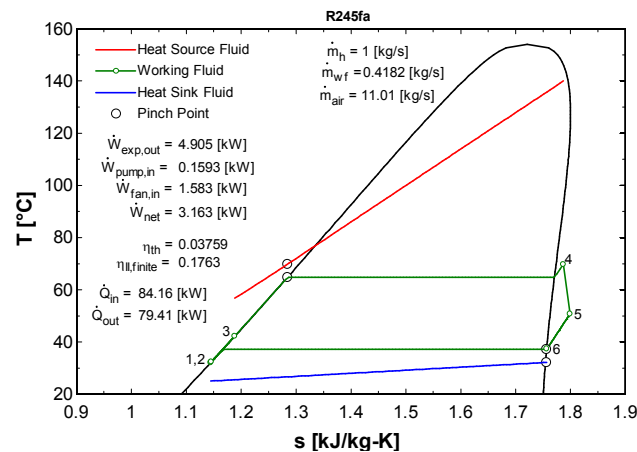


Figure 3: Process diagram for an ORC with low thermal efficiency and high heat recovery. Net power is not optimized. The heat source fluid inlet temperature is 140 °C. Volume-specific cooling fan power is 168 W/(m³/s). Labeled state points correspond to Figure 1.

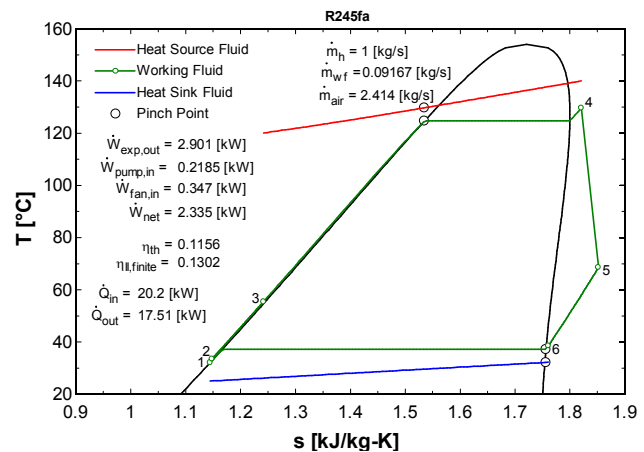


Figure 4: Process diagram for an ORC with high thermal efficiency and low heat recovery. Net power is not optimized, other details as in Figure 3.

In Figure 3, the heat stream is cooled significantly, but it is not utilized effectively due to the low thermal efficiency of the ORC. In Figure 4, the ORC thermal efficiency is high, but less heat can be transferred to the cycle as a result of the higher evaporation temperature. This is contrasted with the case shown in Figure 5, in which the heat recovery and thermal efficiency are optimally balanced to maximize the net power produced. Further gains can be

achieved by changing working fluids. Figure 6 shows how a transcritical ORC can produce more power from the same heat source fluid than the optimized ORC in Figure 5. It achieves this through a better temperature glide match between the heat source fluid and the working fluid.

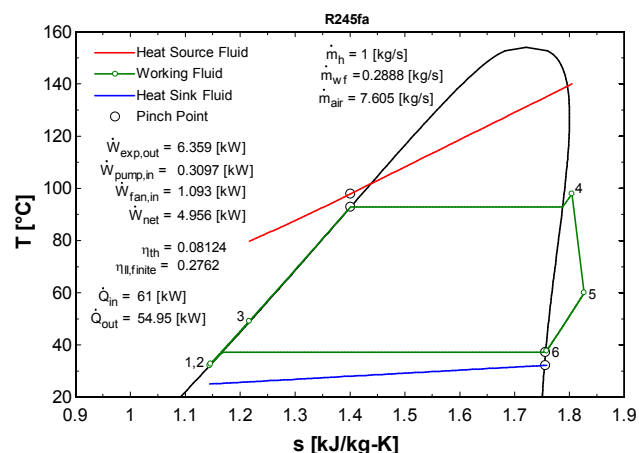


Figure 5: Process diagram for an ORC with net power optimized. Other details as in Figure 3.

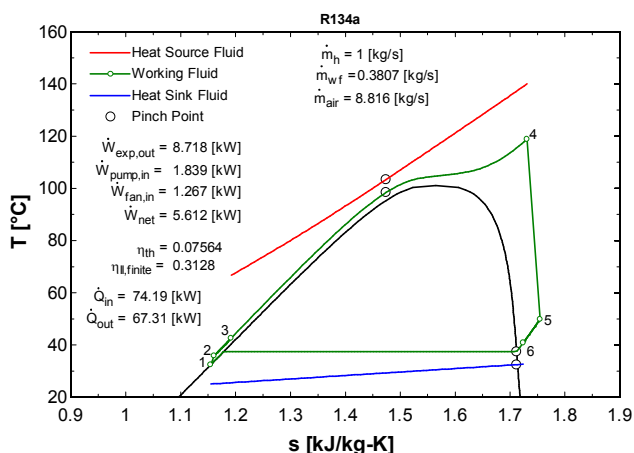


Figure 6: Process diagram for a transcritical ORC with net power optimized. Other details as in Figure 3. The transcritical cycle offers higher net power than the cycle shown in Figure 5.

This illustrates the need to consider cycle configurations that appropriately balance the competing effects of heat recovery and thermal efficiency. In this regard, two alternative ORC configurations that can offer increased power production over traditional ORCs are considered in the present work: the ORC with two-phase flash expansion and the ORC with a zeotropic working fluid mixture (ZRC). It is assumed that both systems receive heat from a single-phase (sensible) heat source and reject heat to air via forced convection. The focus of the present work is to compare the thermodynamic performance of these alternate cycle configurations with that of a baseline ORC. The results are used to determine which cycle configuration has the highest potential for improved performance.

1.1 ORC with Two-Phase Flash Expansion

The ORC with two-phase flash expansion utilizes the same main system components as a traditional ORC, as shown in Figure 1. The main distinction is that the expander inlet state is a saturated liquid or a two-phase mixture with a low vapor quality. A process diagram on the temperature-entropy plane can be seen in Figure 7 for the case of R245fa, where the vapor quality at the expander inlet has been optimized. Note that the optional regenerator has no effect. This cycle approximates the ideal cycle for a sensible heat source: the trilateral cycle. The trilateral cycle has been described formally by Wilson and Radawan (1977). The primary challenge with implementation of such a cycle is the two-phase expansion process shown between states 4 and 5 in Figure 7. This process is best achieved using a positive displacement expander such as a screw or scroll type device. A practical implementation of the trilateral cycle was first proposed for direct expansion of geothermal brine by Sprankle (1973). Similar work was conducted by Steidel *et al.* (1982) using a screw machine as the expander. The concept was studied extensively by Smith *et al.* (1993; 1994), and a means of high-efficiency, low-cost two-phase expansion using twin screw machines was eventually developed (1996; 1998; 1999; 2001; 2011). The particular details, benefits, and challenges associated with this cycle are discussed in Section 3.2.

1.2 ORC with Zeotropic Working Fluid Mixture (ZRC)

The ORC with zeotropic working fluid mixture (ZRC) also utilizes the same system components as a traditional ORC, as shown in Figure 1. The use of a zeotropic mixture results in a non-isothermal phase-change process in the evaporator and the condenser, as shown in Figure 8. This can be advantageous because it can allow for better temperature matching of the sensible heat source and heat sink fluids than what can be achieved with a single-component working fluid.

Two notable works concerning zeotropic mixtures as ORC working fluids are those of Angelino and Colonna di Pailiano (1998, 2000). These works focus on modeling of fluid mixture properties as well as thermodynamic cycle modeling. Angelino and Colonna di Pailiano noted that the overall performance of mixtures in ORCs is comparable

to that of pure fluids if the mean condensation temperature is the same (which they assume in their 1998 work). However, using commercial air-cooled heat exchanger software, they noted that the condensation temperature glide of the mixtures resulted in 50% savings in fan electric power at the cost of 70% more heat exchanger area. A simple economic calculation showed a payback period for the additional heat exchanger surface of about one year (2000).

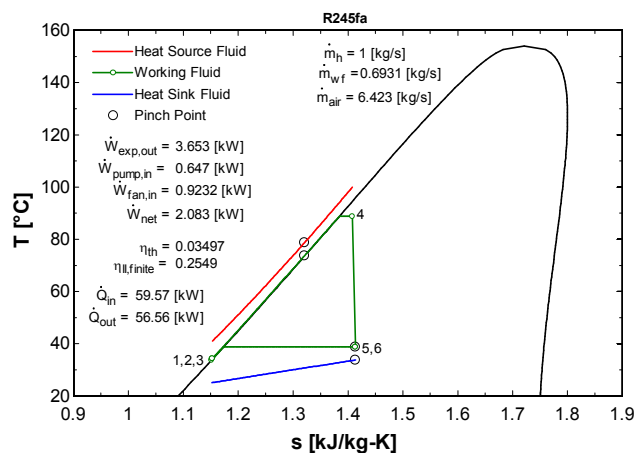


Figure 7: Schematic representation of an ORC with two-phase flash expansion. Other details are the same as in Figure 2.

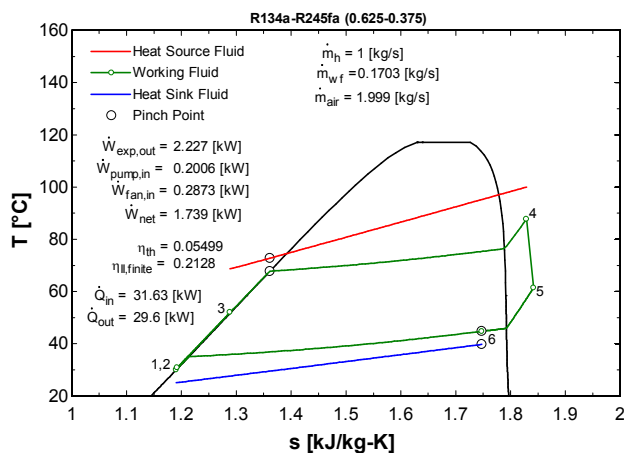


Figure 8: Process diagram of a ZRC. Component concentrations are given on a mass basis. Other details are the same as in Figure 2.

More recently, interest in zeotropic mixtures as ORC working fluids has increased. Works by Chen *et al.* (2011), Heberle *et al.* (2012), and Chys *et al.* (2012) each use simple thermodynamic models to show performance benefits for zeotropic mixtures in ORCs. However, the standards by which such benefits are measured differ among authors. In particular, the criteria of constant average condensing temperature applied across different working fluid mixtures could be problematic. For example, if mixtures with large temperature glides are studied, their minimum condensing temperature could fall below the temperature of the environment. The approach employed in the present work is to use the same minimum condensing temperature and to evaluate the air-side fan power requirement. Evaluation of the fan power captures the benefit of the temperature glide on the low side, which reduces the required air flow rate through the condenser. Details, benefits, and challenges associated with the ZRC are discussed in Section 3.3.

2. MODELING METHODS

Based on the existing body of work, it seems appropriate to develop a basis of comparison for alternative ORC configurations that can describe the performance of each cycle in terms of the available heat input and the required heat rejection capacity at a fixed air inlet temperature. One such method is presented and is applied consistently across multiple cycle configurations and working fluids.

2.1 Heat Exchanger Pinch Points

Most simple thermodynamic ORC models account for irreversibility in the pump and expander by assigning a reasonable value of isentropic efficiency to each component. In this way a pump and expander that are well designed for an application can be modeled without the need to specify and account for their design or geometry. However, the methods of accounting for heat transfer irreversibility in the heat exchangers vary widely. It is desirable to have a means of characterizing heat exchanger performance that parallels the isentropic efficiency model for rotating equipment. The heat exchanger effectiveness is an obvious choice, but its application to multi-zone heat exchangers requires that the maximum possible heat transfer be carefully specified in each case. It also yields different minimum temperature differences for each working fluid and condition. Therefore, a dependent parameter of the heat exchanger effectiveness, the pinch point temperature difference, is used. The pinch point is defined as the minimum temperature difference between the two fluids. In addition, all heat exchangers are assumed to have a counterflow arrangement, which represents an upper limit on heat exchanger performance. As with isentropic efficiency, by selecting a reasonable pinch point, the heat exchanger performance is modeled without specifying its design or geometry. The pinch point model is readily adapted for single-phase, multi-zone, or transcritical heat transfer processes. These two component performance characteristics can be used for

thermodynamic comparison across multiple cycle configurations to get a clear picture of which configuration has the highest thermodynamic potential. The ability of the model to locate heat exchanger pinch points is illustrated in Figures 2 through 8.

A thermodynamic model that utilizes constant values of isentropic efficiency and constant heat exchanger pinch points is good for general thermodynamic comparisons of different cycle configurations and working fluids. However, a more refined comparison requires detailed modeling that incorporates particular component designs and estimates isentropic efficiencies and heat exchanger performance given a working fluid and a set of operating conditions. The economics of designing and manufacturing components to achieve the calculated performance should also be considered.

2.2 Air-Side Condenser Fan Power

Another important feature of the model is the consideration of the fan power required to cool the working fluid in the condenser. With the condenser pinch point assumed, the required air mass flow rate is computed. Then, the condenser fan power is evaluated by

$$\dot{W}_{in, fan} = \frac{\dot{m}_{air} \cdot v_{air} \Delta P_{fan, cond}}{\eta_{fan}} \Rightarrow \frac{\dot{W}_{in, fan}}{\dot{V}_{air}} = \frac{\Delta P_{fan, cond}}{\eta_{fan}}. \quad (1)$$

In this expression, the density of the air is assumed to be constant across the fan. By assuming fan efficiency and pressure drop, the required fan power is estimated. Four pressure drops were chosen to test the sensitivity of each cycle configuration to different fan power requirements without specifying the particular geometry of the condenser. These values can be seen in Table 1.

Table 1: The four air-side pressure drops used to analyze ORC sensitivity to fan power requirements.

$\Delta P_{fan, cond}$ [Pa]	η_{fan}	Volume-Specific Fan Power in W/(m ³ /s) (W/(ft ³ /min)) of air	Comment
0	0.50	0.0 (0.000)	Fan power neglected
50	0.50	100 (0.047)	Lowest value from Yang <i>et al.</i> (2007)
84	0.50	168 (0.079)	Equivalent to $\Delta P_{fan, cond} = 50$ Pa and $\eta_{fan} = 0.30$
423	0.50	846 (0.400)	A standard value for a fully ducted HVAC system

The required condenser fan power is subtracted, along with the pump input power, from the gross expander power to arrive at the cycle net power.

2.3 Performance Metric for a Heat Engine with a Finite Capacity Heat Source

With a method established to model a variety of ORC configurations, it is necessary to select performance criteria against which they will be compared. It is useful to compare the performance of thermal systems against the theoretical maximum performance specified by the Second Law of Thermodynamics. Such a comparison is called the Second Law efficiency, defined as

$$\eta_{II} = \frac{\dot{E}_{recovered}}{\dot{E}_{supplied}} = \frac{\dot{W}_{net}}{\dot{m}_h \int_o^{in} \left(1 - \frac{T_o}{T}\right) \delta q}, \quad (2)$$

where T is the temperature of the heat source fluid, which varies as heat is transferred from the source fluid to the working fluid. For the special case of a constant temperature source fluid and the appropriate choice of integration limits, Equation (2) is readily simplified to yield a ratio of thermal efficiency to the Carnot efficiency. However, for a source fluid of finite heat capacity, neglecting changes in pressure, kinetic energy, and potential energy, Equation (2) becomes

$$\eta_{II, finite} = \frac{\dot{W}_{net}}{\dot{m}_h \left[\int_o^{in} \delta q - T_o \int_o^{in} \frac{\delta q}{T} \right]} = \frac{\dot{W}_{net}}{\dot{m}_h \left[(h_{in} - h_o) - T_o (s_{in} - s_o) \right]}. \quad (3)$$

A useful feature of Equation (3) as an objective function is that, for a heat source fluid of fixed mass flow rate, pressure, and inlet temperature, the denominator is fixed and independent of the cycle configuration. Therefore,

maximization of $\eta_{II,finite}$ is the same as maximization of \dot{W}_{net} . Also, computation of a percent change in $\eta_{II,finite}$ between cycle configurations is the same as the percent change in \dot{W}_{net} .

2.4 Model Parameters and Optimization

The model parameters assumed constant and shown in Table 2 are applied consistently across all cycle configurations studied in this work.

Table 2: Model parameters (and their values) which are held constant over all cycle configurations.

Description	Value
Condenser outlet subcooling	5 K
Heat exchanger pinch point temperature difference	5 K
Dead state temperature, heat sink fluid inlet temperature	25 °C
Pump isentropic efficiency	0.60
Expander isentropic efficiency	0.75
Air-side condenser fan efficiency	0.50

Additional assumptions applicable to each cycle are explained in their respective sections. Heat source fluid inlet temperatures between 80 °C and 200 °C were studied. For each working fluid and source fluid inlet temperature, the remaining system parameters were varied to maximize the Second Law efficiency defined in Equation (3) within the constraints imposed by each cycle configuration. These parameters are 1) working fluid high-side pressure, 2) working fluid low-side pressure, and 3) evaporator outlet superheat. For the baseline ORC and the ZRC, supercritical high-side pressures were allowed, resulting in transcritical cycles for sufficiently high source temperatures. For the ORC with two-phase flash expansion, evaporator superheat was replaced by evaporator outlet quality. For the ZRC, the additional parameter of working fluid mixture concentration was also varied. Optimization was performed using the gradient-based algorithms available in Engineering Equation Solver (Klein, 2012).

2.5 Working Fluids Studied

Table 3 gives the working fluids that were studied for the baseline ORC. These fluids were selected to provide a wide range of critical temperatures and a wide range of wet or dry expansion behavior. A variety of natural, hydrocarbon, and hydrofluorocarbon working fluids are also represented. Thermodynamic properties for these working fluids and mixtures were obtained from REFPROP 9.0 (Lemmon *et al.*, 2012).

2.6 Model Limitations

In general the model is limited in the following ways:

- It does not account for the heat exchanger area that would be required to achieve a 5 K pinch point temperature difference, which changes with average temperature difference and fluid transport properties.
- It does not account for the ease or difficulty of achieving the specified isentropic efficiencies for the pump and expander over different pressure ratios, volume ratios, or vapor quality.
- It does not consider the relative size or speed of the pump and expander that would be required to achieve the needed volumetric flow rates.
- It does not consider the relative size of lines and heat exchangers that would be necessary to minimize pressure losses.
- It does not account for the practical challenges associated with high system pressures (particularly for transcritical cycles) or for sub-atmospheric condensing pressures required by some working fluids.
- It does not account for the auxiliary power or other losses that might be involved in bringing the waste heat source into thermal contact with the working fluid.

These model limitations, while important, do not impact the primary objective of this study, which is to evaluate thermodynamic cycles and fluids that have the highest *potential* for effective waste heat recovery.

Table 3: Working fluids considered in the present study.

Working Fluid	Chemical Name	Chemical Formula	Molecular Weight	Saturated Vapor Line	Critical Temperature [°C]	Critical Pressure [kPa]	Normal Boiling Point [°C]	Condensing Pressure at 35 °C [kPa]
CO ₂ (R744)	carbon dioxide	CO ₂	44.0	wet (transcritical)	31.0	7377	-78.4	N/A
Propane (R290)	propane	C ₃ H ₈	44.1	wet	96.7	4251	-42.1	1220
R134a	1,1,1,2-tetrafluoroethane	C ₂ H ₂ F ₄	102	isotropic (wet)	101	4059	-26.1	887
R227ea	1,1,1,2,3,3,3-heptafluoropropane	C ₃ HF ₇	170	isotropic (dry)	102	2925	-16.3	611
R152a	1,1-difluoroethane	C ₂ H ₄ F ₂	66.1	wet	113	4517	-24.0	794
Ammonia (R717)	ammonia	NH ₃	17.0	wet	132	11330	-33.3	1350
Isobutane (R600a)	2-methylpropane	C ₄ H ₁₀	58.1	isotropic (dry)	135	3629	-11.7	465
R245fa	1,1,1,3,3-pentafluoropropane	C ₃ H ₃ F ₅	134	isotropic (dry)	154	3651	15.1	212
Neo-pentane	2,2-dimethylpropane	C ₅ H ₁₂	72.1	dry	161	3196	9.50	233
Pentane (R601)	pentane	C ₅ H ₁₂	72.1	dry	197	3370	36.1	97.7
Acetone	propanone	C ₃ H ₆ O	58.1	isotropic (wet)	235	4700	56	46.5
Hexane	hexane	C ₆ H ₁₄	86.2	dry	235	3034	68.7	30.6
Water (R718)	water	H ₂ O	18.0	wet	374	22060	100	5.63

3. CYCLE PERFORMANCE AND OPTIMUM WORKING FLUID SELECTION

3.1 Baseline ORC and Working Fluid Selection

The proposed alternate ORC configurations of Sections 1.1 and 1.2 are compared against a baseline ORC to evaluate their merits. The baseline is a typical configuration of a single-fluid ORC. It is represented schematically in Figure 1 with a process diagram shown in Figure 2. The constraints particular to the baseline ORC are given in Table 4. These constraints represent conditions of a conservatively operated expander.

Table 4: Particular constraints to the baseline ORC

Description	Value
Evaporator outlet superheat	≥ 5 K
Expander discharge vapor quality	≥ 0.95

The maximum Second Law efficiency according to Equation (3), for a selection of the working fluids shown in Table 3, is plotted as a function of source fluid inlet temperature in Figure 9. For the results in Figure 9, cooling fan power has been neglected. The values for working fluids studied but not shown in the figure lie within the range of the data presented. It can be seen in Figure 9 that the working fluid which produces the most power from a given heat source fluid flow rate over most source temperatures is R134a. This is primarily due to its relatively low critical temperature, which permits it to operate in a transcritical cycle at source fluid temperatures at or above 140 °C. The higher critical temperature of R245fa does not yield a transcritical cycle at the optimum until the source temperature is at least 200 °C.

Figure 9 reveals the optimal working fluid for the baseline ORC at a given source fluid temperature, with cooling fan power neglected. The alternate ORC configurations, using any working fluid, must perform better than the optimal baseline ORC with the optimal working fluid in order to be thermodynamically superior to the baseline. For the three nonzero condenser fan pressure drops shown in Table 1, the optimization exercise was repeated. This exercise revealed an optimal baseline case for each level of condenser fan power considered. In each case, either R134a or R245fa was shown to be the optimal working fluid for the baseline ORC.

3.2 ORC with Two-Phase Flash Expansion and Working Fluid Selection

The ORC with two-phase flash expansion is modeled by eliminating the constraints of the baseline ORC in Table 4. Then, the evaporator exit state is allowed to vary continuously from superheated vapor through the two-phase region. It is constrained to have a minimum outlet quality of 0.0 (saturated liquid). The expander exit quality remains unconstrained. When the cycle is optimized at each source temperature, the working fluid hierarchy drastically shifts, as shown in Figure 10. Except after the transition to transcritical cycles, all points in Figure 10 involve evaporator exit states with a vapor quality below 1.0. In other words, these points represent ORCs with two-phase flash expansion. The increase in Second Law efficiency is primarily due to higher heat recovery from the source fluid. The temperature glide for the source fluid is now closely matched along the working fluid subcooled liquid line, as can be seen in Figure 7.

It can be seen in Figure 10 that the optimal working fluid for the ORC with two-phase flash expansion is water. This presents a challenge for positive displacement expanders. It is known that, for dry vapor expansion in a positive displacement device, the built-in volume ratio should be approximately equal to the expansion volume ratio of the working fluid (Quoilin *et al.*, 2010; Woodland *et al.*, 2012). In contrast, for flash expansion, Smith *et al.* (1996) report that a built-in volume ratio of 20% – 30% of the overall expansion volume ratio is optimal. However, the volume ratios across the expander for flash expansion of water can be on the order of several thousand. This precludes design of an expander that can achieve the isentropic efficiency assumed in Table 2. Therefore, where water was studied in the ORC with flash expansion, a sufficiently high evaporator exit quality was used to ensure an

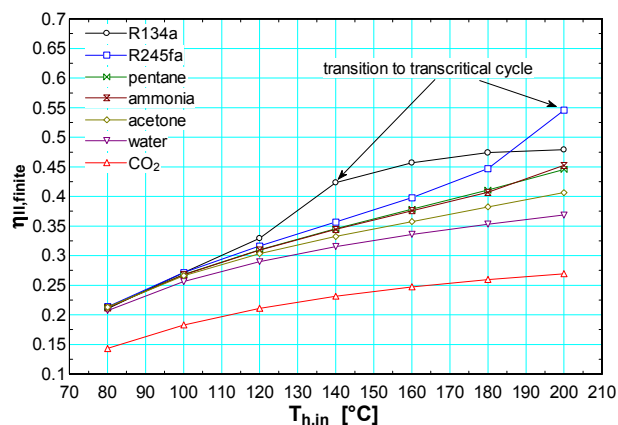


Figure 9: Maximum Second Law efficiency as a function of heat source fluid inlet temperature for the baseline ORC. A selection of the working fluids in Table 3 is shown. Values for working fluids not shown are within the range of the data. Condenser fan power is neglected.

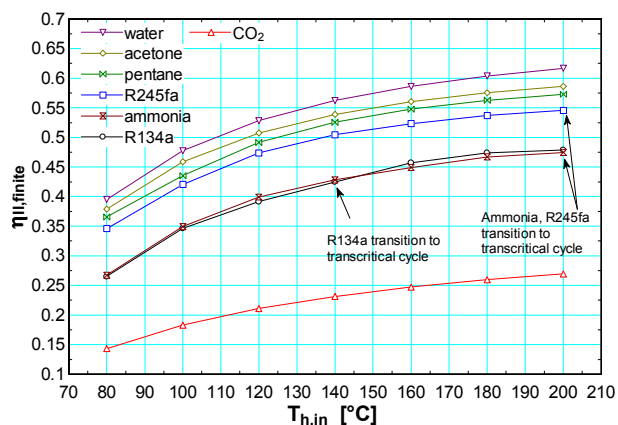


Figure 10: Maximum Second Law efficiency as a function of heat source fluid inlet temperature for an ORC with variable evaporator outlet quality or superheat. Other details are the same as in Figure 9.

expansion volume ratio of less than 160. This indicates a required built-in volume ratio of about 40, which is consistent with the highest expansion ratio indicated for the optimal baseline ORC at a source fluid temperature of 200 °C. It could be achieved in practice by using two positive displacement expanders in series.

3.3 ZRC and Working Fluid Selection

The ZRC is modeled under the same constraints as the baseline ORC, given in Table 4. The working fluid mixtures studied are all binary mixtures, which were formed from the working fluids in Table 3. These mixtures are given in Table 5. Working fluid pairs are listed with the more volatile component first. Concentrations are given on a mass basis in a format that parallels the working pair naming convention. As stated in Section 2.4, the concentration of the working fluid mixture is a design parameter in the optimization of the ZRC. However, to reduce the number of function calls to mixture property routines, the concentration was not varied continuously. Instead, the following discrete values of concentration were allowed: 0.000-1.000, 0.125-0.875, 0.250-0.750, 0.375-0.625, 0.500-0.500, 0.625-0.375, 0.750-0.250, 0.875-0.125, 1.000-0.000. While mixing parameters are not available in REFPROP 9.0 for many of these working pairs, the estimation scheme used in the program works fairly well for mixtures of similar fluids, especially among the refrigerants (Lemmon, 2013). However, it should be noted that the ZRC model is limited by the accuracy of the mixture property estimates.

Of all the working pairs studied, the mixture of R134a with R245fa is, with rare exception, the most efficient. In most of the exceptional cases, the differences in Second Law efficiency between the two mixtures are approximately less than 0.005 and are therefore not meaningful. Because of this, the R134a-R245fa mixture is chosen for discussion and comparison with the baseline ORC.

Practical challenges of the ZRC can include differential holdup, whereby the mixture concentration shifts across the heat exchangers Haberle *et al.* (2012). System charging, charge adjustment, and charge recovery are also less straightforward with mixtures. However, a practical benefit of the ZRC is that it can utilize the same expander designs and geometries that are currently in use for ORCs. The working pressures and volume ratios lie in the same range, and both ORCs and ZRCs involve expansion of pure vapor. Therefore, the potential of a “drop-in” upgrade to existing ORC designs is greater for the ZRC than for the ORC with flash expansion, which requires a specially designed expander in order to be efficient.

Table 5: Working fluid mixtures studied with concentration shown for maximum low-side temperature glide.

Mixture	Maximum Temperature Glide at $T_{\text{bubble}} = 35\text{ }^{\circ}\text{C}$ [K]	Concentration at Max Temperature Glide	Estimated Critical Temperature at Concentration for Max Glide [$^{\circ}\text{C}$]	Estimated Critical Pressure at Concentration for Max Glide [kPa]	Condensing Pressure at $T_{\text{bubble}} = 35\text{ }^{\circ}\text{C}$ [kPa]
Neopentane-Pentane	6.84	0.375-0.625	183	3524	169
Propane-Isobutane	6.89	0.500-0.500	118	4239	865
R245fa-Pentane	7.68	0.375-0.625	186	3804	156
Pentane-Hexane	8.25	0.500-0.500	216	3306	67.5
R227ea-R245fa	9.04	0.375-0.625	137	3623	382
R152a-R245fa	12.1	0.250-0.750	138	4055	463
R134a-R245fa	14.5	0.375-0.625	131	3986	537
Propane-R245fa	32.0	0.125-0.875	137	4544	818
Ammonia-Water	97.3	0.625-0.375	250	17940	731
CO ₂ -Acetone	120	0.375-0.625	157	9269	2760

4. COMPARATIVE RESULTS AND DISCUSSION

A comparison of the ORC with two-phase flash expansion and the ZRC against the optimum baseline ORC is presented. The data can be used to help identify the thermodynamically optimum cycle configuration for a given heat source fluid inlet temperature and condenser fan power requirement. The data is presented as the percent improvement in Second Law efficiency (and net work) over the optimal baseline ORC. This comparison is given in Figure 11. Negative improvements are omitted from all plots in order to highlight the potential benefits of each configuration. For the ORC with flash expansion, an additional plot is given with results for R245fa. This is done to aid in cycle comparisons since R245fa was used in the ZRC fluid mixture and in many of the baseline cases. Also, the absolute Second Law efficiency of the baseline ORC is provided for reference in the lower right pane. The optimal working fluid corresponding to each baseline case is labeled to reinforce the fact that the baseline working fluid changes with source temperature and condenser fan power.

Figure 11 illustrates the enormous relative gains that are possible for both alternative cycle configurations, particularly at lower source temperatures. For the ORC with flash expansion, the greatest improvement is for water at a source temperature of 80 $^{\circ}\text{C}$, where the increase is 84% above the baseline. As the source temperature increases, the baseline ORC fluids become better able to match the source temperature glide by executing a transcritical cycle. This reduces the relative gains of the ORC with flash expansion at higher source temperatures.

The potential for improvement of the ORC with flash expansion at the lowest source temperature of 80 °C is also quite sensitive to fan power requirements. This is particularly true when R245fa is used as the working fluid. This sensitivity is due to the low thermal efficiency of the cycle at this low source temperature. In order to maximize net power output, good glide matching is exploited. This glide matching results in a large heat input at a low thermal efficiency, which means more heat must be rejected for each unit of heat input. When the source temperature is low, the cooling requirements are also a more significant portion of the gross output of the expander. At the highest fan power of 846 W/(m³/s), the improvement of the ORC with flash expansion disappears for 80 °C and 100 °C source temperatures.

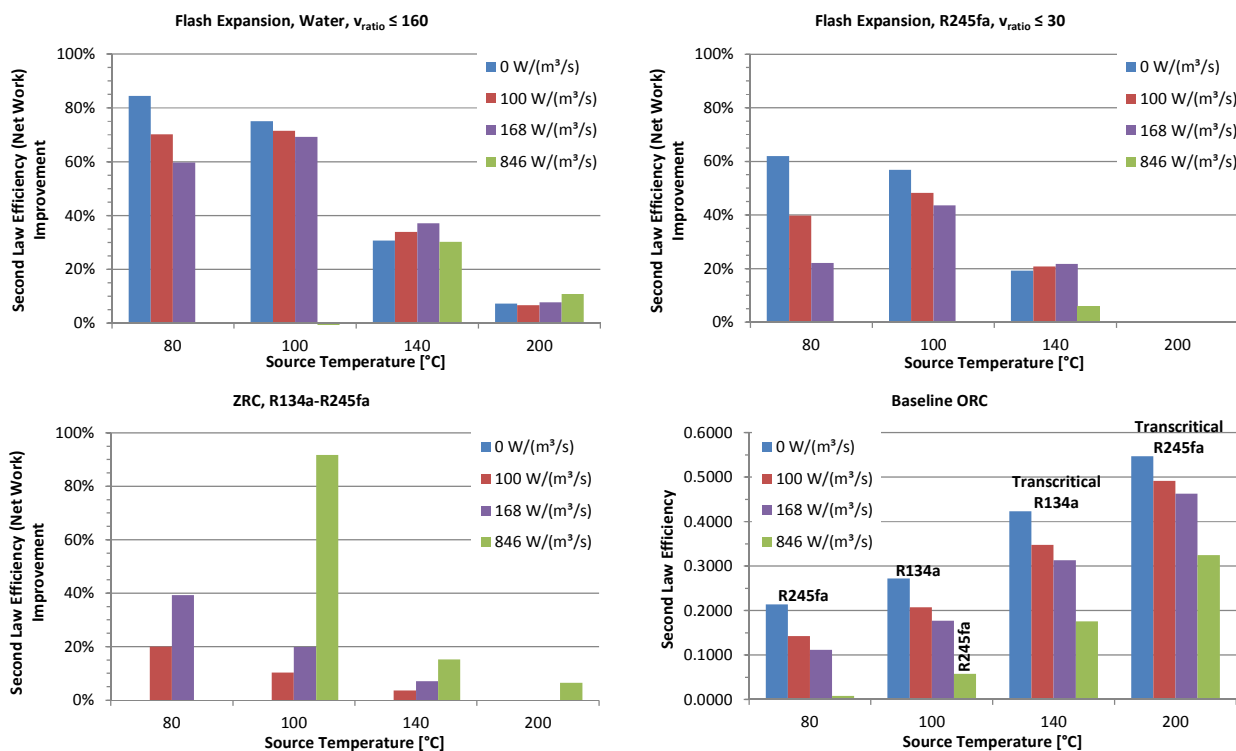


Figure 11: Second Law efficiency (and net work) improvement for the ORC with two-phase flash expansion (using water and using R245fa) and for the ZRC relative to the baseline case. The absolute Second Law efficiency for the baseline ORC is also provided in the lower right pane with the optimal baseline working fluid labeled for each case.

The lower left pane in Figure 11 gives results for the ZRC. When condenser fan power is negligible, the ZRC does not offer any improvement over the baseline. The improvement for the 80 °C source temperature and 846 W/(m³/s) fan power is not shown due to impractically low efficiencies. However, at those conditions, the ZRC shows the best relative improvement with a 277% increase in Second Law efficiency from 0.007875 to 0.02965. In general, the ZRC offers greater improvement at higher fan power and at lower heat source temperatures. The reasons for this can be seen by comparing Figure 8 with Figure 2. For the ZRC, the temperature glide on the low side is steeper than on the high side. This reduces the enthalpy drop across the expander compared to the baseline ORC if the condenser fan power is negligible. An overall benefit only results for nonzero fan power because the low-side temperature glide also reduces the required air flow rate. This simultaneously allows a lower minimum condensing temperature, lower fan power, higher thermal efficiency, and better heat recovery. The benefit is greater when the fan power requirement is a greater proportion of the gross expander output. This occurs at low source temperatures and high volume-specific fan powers.

At a source temperature of 80 °C, even at the lowest nonzero volume-specific fan power, the ZRC shows an improvement of 20%. At a 100 °C source and 846 W/(m³/s) fan power, the improvement is 92%, where the efficiency increases from 0.05734 to 0.1099. At a 200 °C source temperature, the high-side phase change temperature glide is eliminated since the cycle at all concentrations of the working fluid mixture is transcritical. The low-side temperature glide then reduces the expander power by more than the cooling fan power except at the highest fan consumption rate.

From Figure 11, it can be seen that the most potential for improvement over the greatest range of source temperatures and cooling fan power requirements is for the ORC with two-phase flash expansion. This is particularly true if water is used as the working fluid. However, even the more practical R245fa, requiring overall expansion volume ratios less than 30, shows more consistent improvement than the ZRC. The second best overall alternative is the ZRC, which shows the best improvement at the highest fan power. It is also better at an 80 °C source temperature and 168 W/(m³/s) fan power than the two-phase flash ORC with R245fa

5. CONCLUSIONS

The ORC with two-phase flash expansion and the ZRC have been analyzed using a simple thermodynamic model. The model employs a heat exchanger pinch point temperature difference to characterize the irreversibility in the heat exchangers. It can be applied uniformly for single-phase, multi-phase, and transcritical heat transfer processes. This type of model is well-suited to comparing the thermodynamic potential of different cycle configurations and working fluids. However, a more refined decision requires detailed modeling that incorporates component geometry and cost.

Based on the model results, the ORC with flash expansion using water can produce the most power from a given heat source fluid flow rate, unless the condenser fan power requirement is high. However, it may be more difficult or costly to expand two-phase water across the required volume ratios. The ORC with flash expansion using R245fa gives intermediate improvement for the majority of source temperatures and condenser fan power requirements. The ZRC gives less consistent improvement with little benefit at higher source temperatures. However, at low source temperatures and higher condenser fan powers, the improvement for the ZRC is greater than for the ORC with flash expansion. The ZRC also has a practical benefit compared to the ORC with flash expansion because it can utilize the same expander designs as the baseline ORC. A more refined recommendation requires detailed modeling of particular component designs and an economic analysis for a specific application.

NOMENCLATURE

\dot{E}	exergy rate	(kW)	Subscripts
P	pressure	(Pa), (kPa)	<i>II</i> Second Law
\dot{Q}	heat transfer rate	(kW)	<i>air</i> air
T	temperature	(°C)	<i>bubble</i> bubble point
\dot{V}	volumetric flow rate	(m ³ s ⁻¹)	<i>cond</i> condenser
\dot{W}	work rate	(kW)	<i>exp</i> expander
h	specific enthalpy	(kJ kg ⁻¹)	<i>fan</i> fan
\dot{m}	mass flow rate	(kg s ⁻¹)	<i>finite</i> finite heat capacity
q	specific heat transfer	(kJ kg ⁻¹)	<i>h</i> heat source fluid
s	specific entropy	(kJ kg ⁻¹ K ⁻¹)	<i>in</i> input, inlet
v	specific volume	(m ³ kg ⁻¹)	<i>net</i> net output
η	efficiency	(-)	<i>o</i> dead state
			<i>out</i> output, outlet
			<i>pump</i> pump
			<i>th</i> thermal
			<i>wf</i> working fluid

REFERENCES

- Angelino, G., & Colonna di Paliano, P. (1998). Multicomponent working fluids for organic Rankine cycles (ORCs). *Energy*, 23(6), 449-463.
- Angelino, G., & Colonna di Paliano, P. (2000). Organic Rankine cycles (ORCs) for energy recovery from molten carbonate fuel cells. In *Energy Conversion Engineering Conference and Exhibit, 2000.(IECEC) 35th Intersociety (Vol. 2, pp. 1400-1409)*. IEEE.

- Chen, H., Goswami, D. Y., Rahman, M. M., & Stefanakos, E. K. (2011, August). Optimizing energy conversion using organic Rankine cycles and supercritical Rankine cycles. In Proceedings of the ASME 2011 5th International Conference on Energy Sustainability.
- Chys, M., van den Broek, M., Vanslambrouck, B., & De Paepe, M. (2012). Potential of zeotropic mixtures as working fluids in organic Rankine cycles. *Energy*.
- Heberle, F., Preißinger, M., & Brüggemann, D. (2012). Zeotropic mixtures as working fluids in Organic Rankine Cycles for low-enthalpy geothermal resources. *Renewable Energy*, 37(1), 364-370.
- Klein, S. (2012). Engineering Equation Solver, F-Chart Software.
- Lemmon, E. (2013). Answers to Frequently Asked Questions. Retrieved July 9, 2013 from http://www.boulder.nist.gov/div838/theory/refprop/Frequently_asked_questions.htm#MixtureErrorMessages
- Lemmon, E., Huber, M., McLinden, M. (2012). NIST Standard Reference Database 23: Reference Fluid Thermodynamic and Transport Properties-REFPROP, Version 9.0, National Institute of Standards and Technology, Standard Reference Data Program, Gaithersburg.
- Quoilin, S., Lemort, V., & Lebrun, J. (2010). Experimental study and modeling of an Organic Rankine Cycle using scroll expander. *Applied energy*, 87(4), 1260-1268.
- Smith, I. K. (1993). Development of the Trilateral Flash Cycle System: Part 1: Fundamental Considerations. *Proceedings of the Institution of Mechanical Engineers, Part A: Journal of Power and Energy*, 207(3), 179-194.
- Smith, I. K., & da Silva, R. P. M. (1994). Development of the trilateral flash cycle system Part 2: increasing power output with working fluid mixtures. *Proceedings of the Institution of Mechanical Engineers, Part A: Journal of Power and Energy*, 208(2), 135-144.
- Smith, I. K., Stošič, N., & Aldis, C. A. (1996). Development of the Trilateral Flash Cycle System: Part 3: The Design of High-Efficiency Two-Phase Screw Expanders. *Proceedings of the Institution of Mechanical Engineers, Part A: Journal of Power and Energy*, 210(1), 75-93.
- Smith, I. K., & Stošič, N. R. (1998). *U.S. Patent No. 5,833,446*. Washington, DC: U.S. Patent and Trademark Office.
- Smith, I. K., Stošič, N. R., Aldis, C.A., Brasz, J and Sishla, V. (1999). Twin screw expanders in large chiller units. *Proceedings of International Conference on Industrial Compressors and their Systems*, City University, London, September.
- Smith, I. K., Stošič, N., & Kovacevic, A. (2001). Power recovery from low cost two-phase expanders. *TRANSACTIONS-GEOTHERMAL RESOURCES COUNCIL*, 601-606.
- Smith, I. K., Stosic, N., Mujic, E., & Kovacevic, A. (2011). Steam as the working fluid for power recovery from exhaust gases by means of screw expanders. *Proceedings of the Institution of Mechanical Engineers, Part E: Journal of Process Mechanical Engineering*, 225(2), 117-125.
- Sprankle, R. S. (1973). U.S. Patent No. 3,751,673. Washington, DC: U.S. Patent and Trademark Office.
- Steidel, R. F., Weiss, H., Flower, J. E. (1982). Performance characteristics of the Lysholm engine as tested for geothermal power applications in the Imperial Valley. *Journal of Engineering for Power*. 104. 231-240.
- Wilson, S. S., & Radwan, M. S. (1977). Appropriate thermodynamics for heat engine analysis and design. *Int. J. Mech. Eng. Educ*, 5.
- Woodland, B. J., Braun, J. E., Groll, E. A., & Horton, W. T. (2012). Experimental Testing of an Organic Rankine Cycle with Scroll-type Expander. In Proceedings of the International Refrigeration and Air Conditioning Conference at Purdue University. Paper no. 2505.
- Yang, L., Braun, J. E., & Groll, E. A. (2007). The impact of fouling on the performance of filter–evaporator combinations. *International journal of refrigeration*, 30(3), 489-498.

ACKNOWLEDGEMENT

The authors would like to acknowledge the contributions of Abhinav Krishna, who provided many insightful comments during the course of this study.